Radiometric dating of the type-site for *Homo heidelbergensis* at Mauer, Germany

Günther A. Wagner[a,1], Matthias Krbetschek[b], Detlev Degering[c], Jean-Jacques Bahain[d], Qingfeng Shao[d], Christophe Falguères[d], Pierre Voinchet[d], Jean-Michel Dolo[e], Tristan Garcia[e], and G. Philip Rightmire[f]

[a]Geographisches Institut, Universität Heidelberg, D-69120 Heidelberg, Germany; [b]Sächsische Akademie der Wissenschaften, Institut für Angewandte Physik, Technische Universität Bergakademie, D-09596 Freiberg, Germany; [c]Verein für Kernverfahrenstechnik und Analytik Rossendorf, D-01314 Dresden, Germany; [d]Département de Préhistoire du Muséum national d'Histoire naturelle, Unité Mixte de Recherche 7194, Centre National de la Recherche Scientifique, F-75013 Paris, France; [e]Commissariat à l'Energie Atomique, Laboratoire d'Intégration des Systèmes et des Technologies, Laboratoire National Henri Becquerel, F-91191 Gif-sur-Yvette, France; and [f]Department of Human Evolutionary Biology, The Peabody Museum, Harvard University, Cambridge, MA 02138

Edited by Erik Trinkaus, The Washington University, St. Louis, MO, and approved October 6, 2010 (received for review August 27, 2010)

The Mauer mandible, holotype of *Homo heidelbergensis*, was found in 1907 in fluvial sands deposited by the Neckar River 10 km southeast of Heidelberg, Germany. The fossil is an important key to understanding early human occupation of Europe north of the Alps. Given the associated mammal fauna and the geological context, the find layer has been placed in the early Middle Pleistocene, but confirmatory chronometric evidence has hitherto been missing. Here we show that two independent techniques, the combined electron spin resonance/U-series method used with mammal teeth and infrared radiofluorescence applied to sand grains, date the type-site of *Homo heidelbergensis* at Mauer to 609 ± 40 ka. This result demonstrates that the mandible is the oldest hominin fossil reported to date from central and northern Europe and raises questions concerning the phyletic relationship of *Homo heidelbergensis* to more ancient populations documented from southern Europe and in Africa. We address the paleoanthropological significance of the Mauer jaw in light of this dating evidence.

geochronology | paleoanthropology | physical dating | Quaternary

The nomen *Homo heidelbergensis* was given by Otto Schoetensack in 1908 to the newly discovered mandible from Mauer, near Heidelberg, Germany (1) (Fig. 1). Together with the original Neanderthal skullcap and the "*Pithecanthropus*" fossils from Trinil in Java, the Mauer jaw is one of the classic finds of paleoanthropology. It was found on October 21, 1907, at a depth of 24 m in the Grafenrain sand pit, resting in fluvial sediments named the "Mauer sands" (1). These Mauer sands, including sands and gravels, were deposited by the Neckar River in its former course and are subdivided into two distinct units: the "lower sands" and the "upper sands," separated from each other by a clay/silt layer, the "Lettenbank" (Fig. 2). The mandible of *Homo heidelbergensis* was recovered from a 0.1-m-thick gravel layer within the lower sands.

Both sand units are renowned for their rich early Middle Pleistocene mammal fauna that clearly indicate warm climate conditions (2) attributed to two distinct Middle Pleistocene interglacial stages. The good preservation of the mammal bones (2)—and in particular of the human mandible—indicates that they were transported from a nearby fluvial floodplain before becoming embedded in the river deposits (i.e., they have the same geological age as their surrounding sediment layers).

Age estimates for the Mauer mandible have been advanced previously. The Mauer sands are overlain by several Middle and Late Pleistocene glacial loess layers with interstratified interglacial paleosoil horizons, which constrain the age of the fossil to older than *ca.* 350 ka (3). Magnetostratigraphic studies on clay layers below and within the Mauer sands show normal polarity. Thus, they belong to the Brunhes chron and are younger than 780,000 y (3). Mammalian biostratigraphy places the find layer in a young, but not the youngest, interglacial of the Cromerian complex, probably Cromerian IV or Cromerian III (2, 4). The faunal assemblage from the lower sands, including *Elephas antiquus*, *Stephanorhinus hundsheimensis*, *Bison schoetensacki*, and *Cervalces latifrons*, is quite similar to that of the Italian Paleolithic site of Isernia La Pineta, which is contemporaneous with marine isotope stage (MIS) 15, according to $^{39}Ar/^{40}Ar$ dating on sanidine (5). The evolutionary stage of the vole *Arvicola mosbachensis* at Mauer matches or may be slightly less advanced than that at Isernia, indicating that Mauer should be at least as old as the Italian locality (4). Hence, the interglacial represented by the Mauer lower sands is usually correlated with MIS 13 or MIS 15, orbitally tuned dates of 478–533 ka and 563–621 ka, respectively (6). In view of the importance of this site for documenting the appearance of *Homo heidelbergensis* in Europe, more accurate dating is desirable.

The age of terrestrial Quaternary deposits beyond 400 ka is difficult to assess by chronometric dating, particularly when volcanic layers are missing. Earlier attempts to date the Mauer sands, namely by thermoluminescence of feldspar and electron spin resonance (ESR) of quartz as well as uranium-series (US) dating of an elephant tusk, were unsatisfactory (3). In the meantime, chronometric technologies have advanced, particularly in their range applicability. Especially promising are the ESR combined with US (ESR-US) and infrared radiofluorescence (IR-RF) methods.

Results

The IR-RF technique dates the last light-exposure of sediment grains (i.e., their depositional age). Ten samples from six sediment layers were analyzed using a single-aliquot protocol, which yields a series of ages on small subsamples (1 to 2 mg) of potassium feldspar grains (*SI Materials and Methods*). We have calculated 108 dates (10–20 per dated layer) and can minimize errors caused by incomplete reset of the luminescence clock—resulting in age overestimation—due to insufficient light exposure in the fluvial sediment environment (7, 8). Ages of 607 ± 55 ka, 603 ± 56 ka, 554 ± 33 ka, and 502 ± 27 ka were obtained for the lower sands, whereas the upper sands gave ages of 508 ± 50 ka and 420 ± 23 ka (Fig. 3 and Table 1).

Eight herbivore teeth (five from the lower sands and three from the upper sands) were analyzed with the ESR-US technique (9). As reported in a previous study (10), most of the Mauer dental-tissue samples show evidence of postmortem uranium uptake, allowing the calculation of reliable ESR-US ages. However, for five samples (i.e., ≈25% of the material analyzed), determination of the *p*-parameter was not possible, and this quantity was fixed

Author contributions: G.A.W. guided the project and the geological field work; M.K. and D.D. performed the IR-RF analyses; J.-J.B., Q.S., C.F. and P.V. performed the ESR and US analyses; J.-M.D. and T.G. realized the γ irradiations of the tooth enamel samples; G.P.R. placed the Mauer jaw in paleoanthropological context and assessed the evolutionary role of *Homo heidelbergensis*; and G.A.W., M.K., J.-J.B., C.F., and G.P.R. wrote the paper.

The authors declare no conflict of interest.

This article is a PNAS Direct Submission.

[1]To whom correspondence should be addressed. E-mail: gawag-wagner@web.de.

This article contains supporting information online at www.pnas.org/lookup/suppl/doi:10.1073/pnas.1012722107/-/DCSupplemental.

Fig. 1. Mauer mandible, holotype of *Homo heidelbergensis* (1). The two left premolars were lost in the 1940s (photograph: K. Schacherl).

equal to −1 to allow an age calculation. This procedure leads to an apparent systematic underestimation of the ESR-US ages in comparison with the other samples extracted from the same fluvial unit. The results obtained should be treated as minimum ages and cannot be considered in the geochronological interpretation. The ages obtained for the four other teeth are, respectively, 624 +79/−73 and 627 +73/−71 ka for the lower sands and 458 +39/−37 and 502 +43/−41 ka for the upper sands (Fig. 3 and Table 2).

The gravel bed in the Grafenrain section represents the find layer of *Homo heidelbergensis* in terms of bio- and lithostratigraphy, as well as depth in the deposits. The two sand samples Mau 1 and Mau 2 were taken 0.5 m below and above the gravel bed. The error-weighted mean of their respective IR-RF ages (607 ± 55 ka and 603 ± 56 ka) can be calculated (11) and gives the IR-RF sediment age of 605 ± 42 ka for this horizon, which is supported by the ESR-US age of the sample M0507 (624 ± 79 ka), whose depth level matches exactly that of the original find. Assuming that each of these three data represents the actual age of the layer, their weighted mean yields 609 ± 40 ka. These numeric ages assign the interglacial with *Homo heidelbergensis* at Mauer definitely to MIS 15, which is in full accordance with the above-mentioned biostratigraphic and geological evidence. Taking into account that the find layer was deposited in an interglacial stage, the bracketing data of M0503 and Mau 3 give additional support to this correlation (i.e., it is confirmed by a set of five dates).

Discussion

The hypodigm and evolutionary significance of *Homo heidelbergensis* are currently uncertain, but this species is generally considered to be the ancestor of Neanderthals in Europe (12, 13). Apart from the Mauer jaw, a massive tibia and two teeth from Boxgrove (14), numerous skulls and skeletons from Sima de los Huesos (SH) (15, 16), fossils from Arago Cave (17), and a partial jaw from Visogliano (18) have been attributed to *Homo heidelbergensis*. A minimum age for the SH deposits is now reported to be 530 ka (19), whereas specimens from the British, French, and Italian localities are dated at 500 ka or younger. Older material of secure archaeological and stratigraphic provenience is known only from Atapuerca in Spain. A juvenile partial cranium, a young adult hemimandible, teeth, and other bones have been reported from the TD6 level at Gran Dolina, antedating the Brunhes-Matuyama magnetic reversal at 780 ka (20, 21). Additionally, a lower jaw fragment has been recovered from the TE9 level at Sima del Elefante (22). This discovery, 1.2–1.1 Ma in age, represents the oldest human fossil found anywhere in Europe.

A critical question is how the Early Pleistocene groups at Elefante and Gran Dolina may be related to later populations occupying the circum-Mediterranean region and northern Europe. This problem is complex, and it has not been solved as fossils and artifacts continue to accumulate. One view holds that the first humans to reach Europe should be referred to as *Homo antecessor*. Initially, it was thought that this (new) species could be the common ancestor to Neanderthals and *Homo sapiens* (23). However, the hemimandible from TD6 has been described as similar to jaws of Chinese *Homo erectus*, and its morphology is said to cast doubt on any phyletic link with *Homo heidelbergensis* or the Neanderthals (24). Recently it has been claimed that the hominin from Elefante is part of "a population coming from the east" that may be related to expansion "out of Africa" (25). At the Atapuerca localities, *Homo antecessor* occurs with core and flake tools (a mode 1 industry). Carbonell et al. (24) argue that these Early Pleistocene people were replaced during the Middle Pleistocene by *Homo heidelbergensis*. The latter species, ascribed an African origin, is associated at SH and Boxgrove with Acheulean (mode 2) hand axes.

Such a model, invoking replacement of species equipped with different lithic industries, provides one perspective on the European record. However, given the new date for the Mauer mandible, along with confirmation of 700 ka (or greater) as the age for a mode

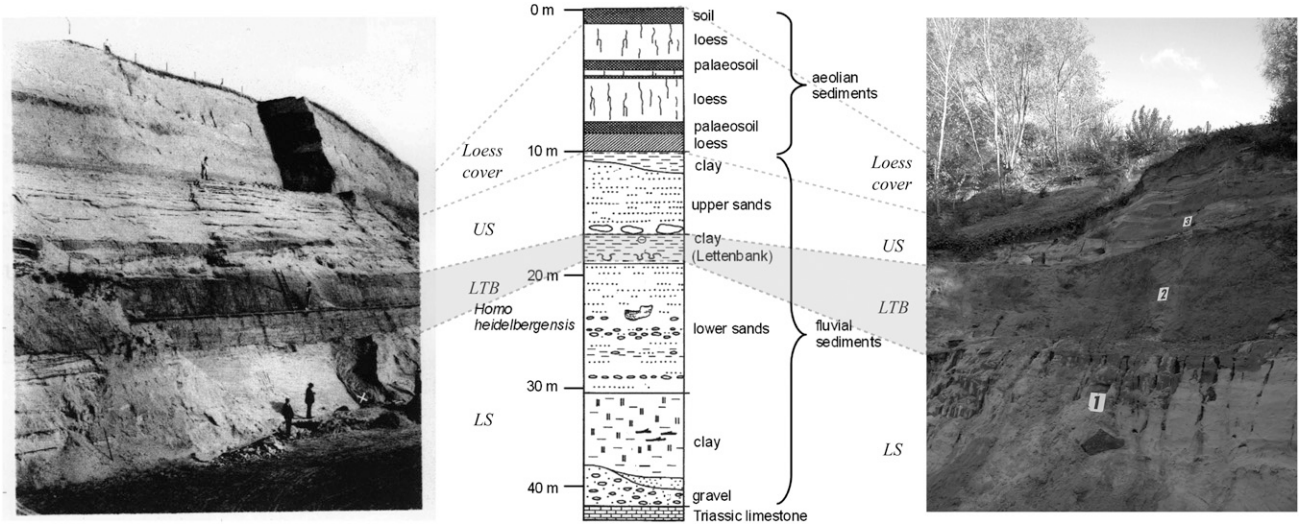

Fig. 2. Stratigraphy of the sand pit Grafenrain at Mauer with the find horizon of the *Homo heidelbergensis* mandible in the lower sands. Left photograph is taken from the original monograph (1), with the find site (x); right photograph shows the present exposure.

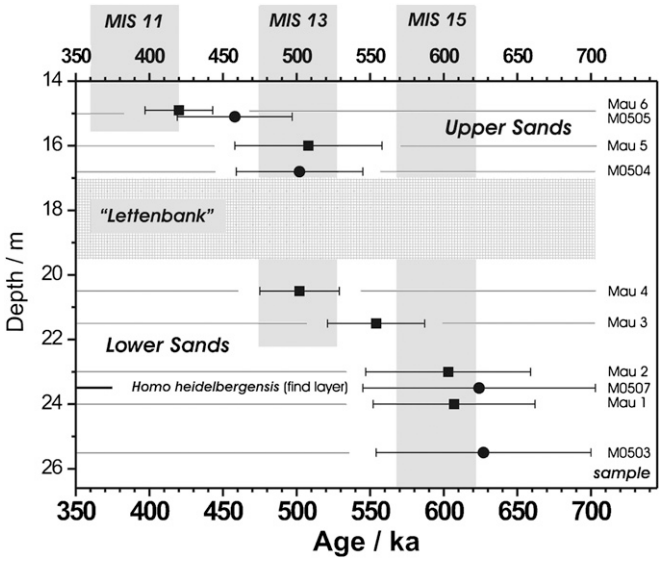

Fig. 3. IR-RF ages (squares) and ESR-US ages (circles) with their 1-σ error bars (± SEM) of samples from the sand pit Grafenrain at Mauer

1 assemblage at Pakefield in Britain (26), it is clear that hominins were colonizing northern Europe less than 100 ka, after the TD6 occupation at Gran Dolina. The gap between early sites in the south and trans-Alpine settlements is narrowing steadily. It is appropriate to question whether there is enough evidence to set the TD6 assemblage apart from the materials discovered at Mauer, SH, and Arago. The number of *Homo antecessor* fossils is still quite small, and several of the craniodental remains are fragmentary and/or subadult. The young adult hemimandible from Gran Dolina (ATD6-96) is described as a probable female with a low corpus, little surface relief, and a steeply inclined alveolar planum. This specimen is said to exhibit a "primitive structural pattern" and to lack apomorphies of European Middle/Late Pleistocene hominins (24). The ATD6-96 corpus is indeed low relative to that of the Mauer, Arago, and SH adults, although it does not differ greatly in "robusticity" (thickness/height) measured at M_1. In recent humans, and presumably in earlier Pleistocene populations, the mandible continues to increase in height during the juvenile period and later into adult life. For all groups, corpus proportions and surface relief show much individual variation. Such traits do not unambiguously differentiate the Gran Dolina hominins from Middle Pleistocene specimens (27). Archaeological traces do not help to clarify this picture. Elefante TE9 and Gran Dolina TD6 contain core and flake tools, but this is the case also at later localities, such as Pakefield, Isernia, Arago, and Bilzingsleben. Beyond confirming that the most ancient Europeans did not make (or discard) hand axes in significant quantities, this pattern is of little help in tracking dispersal routes or establishing population relationships.

Table 1. Position and mean IR-RF ages (±SEM) of the Mauer sediment samples

Mauer units	Sample	Depth (m)	Depth vs. Lettenbank	Age (ka)
Upper sands	Mau 6	15.0	+2.0 m	420 ± 23
	Mau 5	16.0	+1.0 m	508 ± 50
Lettenbank				
Lower sands	Mau 4	20.5	−1.0 m	502 ± 27
	Mau 3	21.5	−2.0 m	554 ± 33
	Mau 2	23.0	−3.5 m	603 ± 56
	Mau 1	24.0	−4.5 m	607 ± 55

In our view, the European record remains difficult to interpret. Several waves of settlement have been claimed, but it is possible that *Homo heidelbergensis* as a paleospecies/lineage is deeply rooted in the Early Pleistocene. Evidence for any Middle Pleistocene replacement is weak. It is apparent that approximately 600 ka, occupations became more numerous in central and northern Europe, probably signaling an increase in population size as humans grew more skilled at coping with challenging environments. After approximately 400 ka, fossils such as Swanscombe display Neanderthal characters (28). At Bilzingsleben (29, 30) and Ceprano (31), which may be penecontemporary with Swanscombe, skull fragments suggest a less specialized morphology. Neanderthals are known to have occupied much of Europe in the later part of the Pleistocene, but whether they coexisted with other populations during the interval between 400 ka and 40 ka is presently uncertain.

Materials and Methods

Dating Methods. The IR-RF and ESR-US methods both use principles of radiation dosimetry to determine the time since their last exposure to light or heat and the formation of minerals, respectively. The RF and ESR signals change with the natural ionizing radiation dose, and thus with time. The equivalent dose (*DE*) and the dose rate (annual dose) are determined in a series of analytical steps. The age is then obtained from the ratio of the *DE* to the annual dose. Different materials and events are dated (i.e., the deposition of the Mauer sands by IR-RF and the formation of mammal teeth by ESR-US). The methods therefore deliver independent results.

IR-RF Dating. The IR-RF technique is one of the physical dating methods that uses luminescence phenomena and radiation dosimetry to determine the time when minerals were last exposed to light or heat (7). More widely known are optically stimulated luminescence (OSL) and thermoluminescence (TL) dating, which follow the same basic principles (i.e., after a reset of the "luminescence clock" by the event to be dated, the luminescence signal changes as a function of the absorbed radiation dose because of charge transfer and storage at defects within the crystal lattice). The radiation field is provided by the decay of natural radioisotopes and cosmic rays.

Because the dose determination differs from that used for other luminescence dating methods, and the underlying phenomenon is unequivocally a fluorescence effect, IR-RF dating was later renamed from "radioluminescence" to "radiofluorescence" (32). IR refers to the emission measured in the near infrared (865 nm), which is characteristic for potassium feldspar (microcline, orthoclase). The physical background and radiation dose dependence of this phenomenon have been intensively investigated, along with the methodological aspects of dating Quaternary sediments (8, 32, 33). Of particular interest for the data presented here is the long-term stability of the IR-RF signal. Age underestimation is observed frequently in OSL and TL dating of feldspar owing to a lack of signal stability. However, this is not the case for IR-RF. Using a regenerative dose procedure, it is possible to obtain IR-RF ages in agreement with independent age controls back to ≈300 ka (34). Furthermore, long-term signal stability is supported by a series of physical experiments (7, 33).

ESR-US Dating. Application of ESR-US dating to herbivore teeth (9, 35, 36) implies consideration of the evolution of the dose rate over time as a result of postmortem uranium incorporation, through the calculation of a specific U-uptake parameter (*p*-parameter) for each dental tissue, except for samples showing evidence of uranium loss. Such a combined approach provides a single age for each tooth, considering all of the analytical data. Age estimates depend on evaluation of the uranium uptake rate that occurred over the burial history of the sample, whereby the main difficulty arises from the postmortem incorporation of uranium causing a change of the dose rate emitted by the different tissues constituting the tooth. Different models of U-incorporation kinetics, such as early uptake and linear uptake (10, 37), were first proposed to calculate ESR ages. The ESR-US approach taking into account both ESR and US data (radioelement contents, isotopic ratios, paleodoses, external γ-dose rate) allows a better description of uranium incorporation into the different dental tissues, as well as the determination of a single age for each sample, through the calculation of an uptake parameter *p* for each tissue (38). The application of this combined approach to materials from archeological and paleontological contexts now allows us to obtain reliable geochronological data for the entire Middle Pleistocene (21, 39). However, the method is not useful when samples exhibit evidence of uranium loss or lie beyond the geochronological limit of application for the US analytical protocol (40).

Table 2. Position and ESR-US ages (±SEM) of the Mauer teeth samples

Sample	Depth vs. Lettenbank	Tissue	*P* value	*DE* (Gy)	Dose rate (μGy/a)	Age (ka)
M0502	4 m	Dentin	−1.00*			
		Enamel	−1.00*	809.7 ± 30.6	2,088 ± 136	388 ± 29
M0505	+2 m	Dentin	−0.11 ± 0.18			
		Enamel	−0.26 ± 0.16	643.6 ± 10.7	1,404 ± 134	458 +39/−37
M0504	+0 m	Dentin	−0.45 ± 0.11			
		Enamel	−0.49 ± 0.13	754.8 ± 23.0	1,504 ± 140	502 +43/−41
Lettenbank						
M0506	−3 m	Dentin	−0.91 ± 0.07			
		Enamel	−0.62 ± 0.14	662.8 ± 13.1	1,478 ± 288	448 +57/−42
		Cement	−1.00*			
M0507	−4 m	Dentin	−0.43 ± 0.11			
		Enamel	−0.40 ± 0.17	813.8 ± 18.5	1,305 ± 199	624 +79/−73
M0508	−5 m	Dentin	−0.39 ± 0.26			
		Enamel	−0.53 ± 0.24	482.6 ± 12.2	1,095 ± 214	441 +73/−34
		Cement	−1.00*			
M0501	−5 m	Dentin	−1.00*			
		Enamel	−0.60 ± 0.37	499.9 ± 46.2	1,037 ± 202	482 +97/−49
M0503	−6 m	Dentin	+0.42 ± 0.25			
		Enamel	+0.63 ± 0.30	676.7 ± 12.7	1,080 ± 133	627 +73/−71

**P* values were limited to −1 (early uptake assumption).

Samples. Ten sand samples were taken from the Grafenrain sand pit in November 2005, from a freshly cleaned wall exposing the sedimentary sequence. The sampled profile is not the one exposed in 1907 at the original, now inaccessible, discovery site. It is situated *ca.* 100 m to the north but exposes the same stratigraphy. Black light- and water-tight plastic tubes (diameter 5 cm) were used for taking samples. To make sure that sufficient material of grain size 100–300 μm would be available, for Mau 1, 2, 5, and 6 two samples were taken in parallel from each horizon, within a distance of 30–40 cm (Table S1). These samples were labeled with the extension Mau x-1 and Mau x-2, respectively. In addition, at each position approximately 1.5 kg of sediment adjacent to the sampling sites was taken for radioisotope analyses. For dose rate determination, analyses of the natural radionuclide contents were performed by γ-ray spectrometry at the Institute of Applied Physics of the Technische Universität Freiberg and the underground laboratory Felsenkeller of the Verein für Kernverfahrenstechnik und Analytik Dresden (Table S1). At both institutions, samples were stored in radon-tight containers for 2 wk before measurement, to reach radioactive equilibrium between ^{226}Ra and ^{222}Rn, which is analyzed by its short-lived daughter nuclides. For details see *SI Materials and Methods*.

Age and error calculations (11) were carried out. The determination of ≈20 IR-RF ages for a sediment layer allows statistical treatment of the data, mainly to reduce errors due to insufficient signal reset at the time of sediment deposition (Fig. S1 and S2) (7, 8). The single aliquot data and ages are listed in Tables S2 and S3, summarized for the sediment horizon when more than one subsample was investigated. These single-aliquot IR-RF age data include all dose rate errors discussed above, the random errors of the equivalent-dose determination procedure, and an additional systematic error of 2% for dose calibration (*SI Materials and Methods*).

Apart from the sand samples (for IR-RF), herbivore teeth (for ESR-US) were selected from the "Mauer collection" in the Staatliches Museum für Naturkunde at Karlsruhe (Table S4). These fossils were collected in the early 1930s, actually much closer to the original discovery site, with known positions relative to the Lettenbank. The depth levels of all samples are shown in Table 2. The tissues (enamel, dentin, and cement) of each tooth were separated and cleaned mechanically using a dental drill. Enamel was then ground and sieved. Nine enamel aliquots (each ≈100 mg) of the 100- to 200-μm grain-size fraction were irradiated, respectively, at doses of 320, 500, 800, 1,250, 2,000, 3,200, 5,000, 8,000, and 12,500 Gy, using a calibrated ^{60}Co γ-ray source (Irradiateur Biologique de Laboratoire source; Laboratoire National Henri Becquerel, Commissariat à l'Energie Atomique Saclay). ESR signal intensities of irradiated and natural aliquots were measured by an EMX Bruker X-band spectrometer, with the following measurement conditions: 10 mW microwave power, 0.1 mT amplitude modulation, 10 mT scan range, 80 ms time constant, and 100 kHz modulation frequency, for three repeated measurements. The equivalent doses *DE* were determined from the asymmetric enamel signal at g = 2.0018 by the additive method, using an exponential fitting (41, 42).

US analyses were made for each dental tissue. Samples (0.1–3 g) were dissolved in HNO_3 and spiked with ^{232}U/^{228}Th. U and Th were separated using an anion exchange resin column (Dowex 1 × 8; 100–200 mesh) in HCl form. Before extracting U and Th with thenoyltrifluoroacetone/benzene solution, isopropyl ether ($C_6H_{14}O$) was used to remove iron from U-bearing solution, and a second anion exchange resin column in HNO_3 form was used to isolate Th. The analyses of purified U and Th were performed by α-ray spectrometry. ESR/US ages were calculated with the ESR-DATA program (36), using an α efficiency (43) of 0.13 ± 0.02 and Monte Carlo β attenuation factors based on the thickness of the tooth enamel with outer layers removed (44). In addition, water content was estimated to be 3 wt% in the enamel, 10 wt% in the dentin and cement. The external γ and cosmic dose rates were evaluated the same way as for the IR data.

US and ESR age data obtained on Mauer teeth are shown in Table 2 and additional analytical data in Tables S5 and S6. U contents of Mauer dentins, cements, and enamels range between 50 and 107 ppm, 14 and 40 ppm, and 0.4 and 3 ppm, respectively. In each tooth, consistent ^{234}U/^{238}U activity ratios are observed in dental tissues. Spectacularly, M0503, the deepest sample recovered from 6 m below Lettenbank, exhibits the highest ^{234}U/^{238}U for each tissue (1.782–1.896). All of the others cluster between 1.332 and 1.589, without apparent variation with stratigraphy. ^{230}Th/^{234}U ratios of M0502, M0505, M0504, and M0507, in order of depth, are similar in different tissues. Most of these dental tissues show evidence of postmortem uranium uptake, and determination of *p*-parameters is possible. Reliable ESR series ages can be calculated. However, ^{230}Th/^{234}U ratios are beyond equilibrium value of one for five tissues (M0502 dentin and enamel, M0501 dentine, and M0506, M0508, and M0501 cements) (Fig. S3).

ACKNOWLEDGMENTS. We thank Rainer Grün for helpful discussions on ESR-US data and age calculations; Norbert Mercier for his help in the dose rate determination for the teeth; Bassam Ghaleb for assistance in the U-series data interpretation; Sepp Unterricker for γ-spectrometry measurements; Manfred Löscher and Erich Mick (*Homo heidelbergensis* von Mauer e.V.) for support of the field work; and Dieter Schreiber and Eberhard Frey (Staatliches Museum für Naturkunde Karlsruhe) for supplying the teeth samples. Régions "Ile de France" and "Centre" provided financial support in the acquisition of the electron spin resonance and γ-spectrometers of the Museum National d'Histoire Naturelle.

1. Schoetensack O (1908) *The Mandible of Homo Heidelbergensis from the Sands of Mauer near Heidelberg—A Contribution to the Palaeontology of Man* (Engelmann, Leipzig) (in German).

2. von Koenigswald W (1992) On the ecology and biostratigraphy of both Pleistocene faunas of Mauer near Heidelberg. *The Strata of Mauer—85 Years Homo erectus heidelbergensis*, eds Beinhauer KW, Wagner GA (Braus, Mannheim), pp 101–110 (in German).

3. Wagner GA, Fezer F, Hambach U, von Koenigswald W, Zöller L (1997) The age of *Homo heidelbergensis* of Mauer. *Homo heidelbergensis of Mauer—The Appearance of Humans in Europe*, eds Wagner GA, Beinhauer KW (Winter, Heidelberg), pp 124–143 (in German).
4. Wagner GA, Maul LC, Löscher M, Schreiber HD (2010) Mauer—the type site of *Homo heidelbergensis*: Palaeoenvironment and age. *Quat Sci Rev* 10.1016/j.quascirev.2010.01.013.
5. Coltorti M, et al. (2005) New $^{40}Ar/^{39}Ar$, stratigraphic and palaeoclimatic data on the Isernia La Pineta Lower Palaeolithic site, Molise, Italy. *Quaternary Int* 131:11–22.
6. Liesiecki LE, Raymo MEA (2005) A Pliocene-Pleistocene stack of 57 globally distributed benthic $\delta^{18}O$ records. *Paleoceanography* 20:PA1003, 10.1029/2004PA001071.
7. Wintle A (2008) Luminescence dating: Where it has been and where it is going. *Boreas* 37:471–482.
8. Krbetschek MR, Trautmann T, Dietrich A, Stolz W (2000) Radioluminescence dating: Methodological aspects. *Radiat Meas* 32:493–498.
9. Grün R, Schwarcz HP, Chadam JM (1988) ESR dating of tooth enamel: Coupled correction for U-uptake and U-series disequilibrium. *Nucl Tracks Radiat Meas* 14:237–241.
10. Ikeya M (1982) A model of linear uranium accumulation for ESR age of Heidelberg (Mauer) and Tautavel bones. *Jpn J Appl Phys* 22:L763–L765.
11. Aitken MJ (1985) *Thermoluminescence Dating* (Academic Press, London).
12. Stringer C (2002) Modern human origins: Progress and prospects. *Philos Trans R Soc Lond B Biol Sci* 357:563–579.
13. Rightmire GP (1998) Human evolution in the Middle Pleistocene: The role of *Homo heidelbergensis*. *Evol Anthropol* 6:218–227.
14. Stringer CB, Trinkaus E, Roberts MB, Parfitt SA, Macphail RI (1998) The Middle Pleistocene human tibia from Boxgrove. *J Hum Evol* 34:509–547.
15. Arsuaga JL, Martínez I, Gracia A, Carretero JM, Carbonell E (1993) Three new human skulls from the Sima de los Huesos Middle Pleistocene site in Sierra de Atapuerca, Spain. *Nature* 362:534–537.
16. Arsuaga JL, Martínez I, Gracia A, Lorenzo C (1997) The Sima de los Huesos crania (Sierra de Atapuerca, Spain). A comparative study. *J Hum Evol* 33:219–281.
17. de Lumley H, de Lumley MA, Fournier A (1982) The mandible of the human of Tautavel. *1er Congrès International de Paléontologie Humaine, Nice*, ed CNRS (France), pp 178–221 (in French).
18. Abbazzi L, et al. (2000) New human remains of archaic *Homo sapiens* and Lower Palaeolithic industries from Visogliano (Duino Aurisina, Trieste, Italy). *J Archaeol Sci* 27:1173–1186.
19. Bischoff JL, et al. (2007) High-resolution U-series dates from the Sima de los Huesos hominids yields 600 +∞/−66 kyrs: Implications for the evolution of the early Neanderthal lineage. *J Archaeol Sci* 34:763–770.
20. Parés JM, Pérez-González A (1995) Paleomagnetic age for hominid fossils at Atapuerca archaeological site, Spain. *Science* 269:830–832.
21. Falguères C, et al. (1999) Earliest humans in Europe: The age of TD6 Gran Dolina, Atapuerca, Spain. *J Hum Evol* 37:343–352.
22. Carbonell E, et al. (2008) The first hominin of Europe. *Nature* 452:465–469.
23. Bermúdez de Castro JM, et al. (1997) A hominid from the lower Pleistocene of Atapuerca, Spain: Possible ancestor to Neandertals and modern humans. *Science* 276:1392–1395.
24. Carbonell E, et al. (2005) An Early Pleistocene hominin mandible from Atapuerca-TD6, Spain. *Proc Natl Acad Sci USA* 102:5674–5678.
25. Martinón-Torres M, et al. (2007) Dental evidence on the hominin dispersals during the Pleistocene. *Proc Natl Acad Sci USA* 104:13279–13282.
26. Parfitt SA, et al. (2010) Early Pleistocene human occupation at the edge of the boreal zone in northwest Europe. *Nature* 466:229–233.
27. Rightmire GP (2008) Homo in the Middle Pleistocene: Hypodigms, variation, and species recognition. *Evol Anthropol* 17:8–21.
28. Stringer CB, Hublin J-J (1999) New age estimates for the Swanscombe hominid, and their significance for human evolution. *J Hum Evol* 37:873–877.
29. Vlček E (1999) The fossil human of Bilzingsleben: Reconstruction of the skull, the morphology and the taxonomic-phylogenetic position. *Praehist Thuringia* 3:11–26 (in German).
30. Mallik R, Frank N, Mangini A, Wagner GA (2001) Precise Th/U-dating of archaeologically relevant travertine occurences of Thuringia. *Early Humans in Middle Europe—Chronology, Culture, Environment*, eds Wagner GA, Mania D (Shaker, Aachen), pp 77–89 (in German).
31. Muttoni G, Scardia G, Kent DV, Swisher CC, Manzi G (2009) Pleistocene magnetochronology of early hominin sites at Ceprano and Fontana Ranuccio, Italy. *Earth Planet Sci Lett* 286:255–268.
32. Erfurt G, Krbetschek MR (2003) Studies on the physics of the infrared radioluminescence of potassic feldspar and on the methodology of its application to sediment dating. *Radiat Meas* 37:505–510.
33. Erfurt G (2003) Infrared luminescence of Pb^{+} centres in potassium-rich feldspars. *Phys Status Solidi* 200:429–438.
34. Degering D, Krbetschek MR (2007) *The Climate of Past Interglacials*, eds Sirokko F, Claussen M, Sanchez Goni MF, Litt T (Elsevier, Amsterdam), pp 157–172.
35. Bahain JJ, Yokoyama Y, Falguères C, Sarcia MN (1992) ESR dating of tooth enamel: A comparison with K-Ar dating. *Quat Sci Rev* 11:245–250.
36. Grün R (2009) The DATA program for the calculation of ESR age estimates on tooth enamel. *Quat Geochronol* 4:231–232.
37. Bischoff JL, Rosenbauer RJ (1981) Uranium series dating of human skeletal remains from the Del Mar and Sunnyvale sites, California. *Science* 213:1003–1005.
38. Falguères C, Bahain JJ, Saleki H (1997) U-series and ESR dating of teeth from Acheulian and Mousterian levels at La Micoque (Dordogne, France). *J Archaeol Sci* 24:537–545.
39. Bahain J-J, et al. (2007) ESR chronology of the Somme River Terrace system and first human settlements in Northern France. *Quat Geochronol* 2:356–362.
40. Grün R, Aubert M, Hellstrom J, Duval M (2010) The challenge of direct dating old human fossils. *Quatern Int* 223–224:87–93.
41. Grün R (1989) Electron spin resonance (ESR) dating. *Quatern Int* 1:65–109.
42. Yokoyama Y, Falguères C, Quaegebeur JP (1985) ESR dating of quartz from quaternary sediments: First attempt. *Nucl Tracks Radiat Meas* 10:921–928.
43. Grün R, Katzenberger-Apel O (1994) An alpha irradiator for ESR dating. *Ancient TL* 12:35–38.
44. Marsh RE, Prestwich WV, Rink WJ, Brennan BJ (2002) Monte Carlo determinations of the beta dose rate to tooth enamel. *Radiat Meas* 35:609–616.